

Relativistic Density Functional Theory Study of Dioxoactinide(VI) and -(V) Complexation with Alaskaphyrin and Related Schiff-Base Macrocyclic Ligands

Grigory A. Shamov and Georg Schreckenbach*

Department of Chemistry, University of Manitoba, Winnipeg, Manitoba, Canada, R3T 2N2

Received: May 18, 2006

Formation of complexes of alaskaphyrin **1**, bi-pyren **2** and bi-tpmd **3** ligands with actinyl ions AnO_2^{n+} , $An = U, Np, Pu$ and $n = 1, 2$, was studied using density functional theory (DFT) within the scalar relativistic four-component approximation. The alaskaphyrin complexes of the uranyl are predicted to have a bent conformation, in contrast to the experimentally available X-ray data. This deviation is likely due to crystal packing effects. Apart from these conformational differences, calculated geometry parameters and vibrational frequencies are in agreement with the available experimental data. The character of bonding in the complexes is investigated using bond order analysis and extended transition states (ETS) energy decomposition. Metal-to-ligand bonds can be described as primarily ionic although substantial charge transfer is observed as well. Based on ETS analysis, it is shown that steric and/or *fit/misfit* requirements of actinyl cations to the ligand cavities, among the studied complexes, are the most favorable for the bi-pyren ligand **2**, because its flexibility allows for optimal metal-to-donor-atom distances. Planarity of the equatorial coordination sphere of the actinide atom is found to be less important than the ability of a ligand to provide optimal uranium-to-nitrogen bond lengths. Experimental differences in demetalation rates between similar alaskaphyrin, bi-pyren and bi-tpmd uranyl complexes are explained as a result of easier protonation of the Schiff-base nitrogen of the latter. Reduction potentials calculated for the uranium complexes show a good agreement with the experiment, both in relative and in absolute terms.

Introduction

Complexes of the actinides are of both fundamental and practical interest. Actinides found practical use in the nuclear energy industry, which is and will probably remain one of the major suppliers of energy. Therefore, issues related to nuclear fuel reprocessing and nuclear waste storage have to be addressed. In addition, there are other environmental problems and threats, from contaminated sites of the Cold War to “dirty bombs” hazards.

Nuclear waste typically contains both actinides (mostly U, Np, Pu, Am) and their fission products (lanthanides, Cs, Tc) in an aqueous environment. The treatment of nuclear waste involves either separation of the actinides as useful commodities (for reuse as nuclear fuel, for example) or their immobilization for further storage.

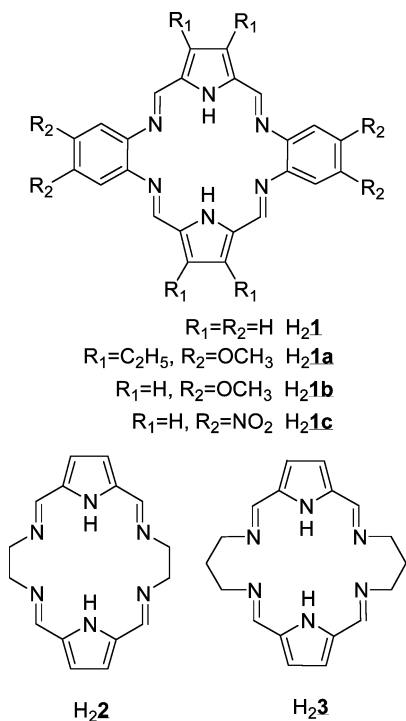
In aqueous solutions, uranium and neptunium complexes exist mostly in the form of actinyl cations AnO_2^{n+} (with $n = 2$ for uranium and 1 for neptunium, correspondingly). Under similar conditions, for plutonium in solution there is a complicated equilibrium of plutonyls(V) and -(VI) and complexes of plutonium(IV). The actinyl moiety is remarkable due to the fact that it is, in contrast to similar d-element compounds, linear and has very short metal-to-oxygen bond lengths, suggesting a strong multiple bond character. Actinyl complexes normally coordinate 4–6 monodentate ligands in their equatorial plane. The f-elements, in contrast to transition metals, are in general *hard* acids and therefore have the strongest affinity to *hard* O-, F-donor ligands. For that reason, there are only a few ligands that are able to compete with water itself. One of the methods

proposed for nuclear waste treatment involves the coordination of actinide ions with polydentate macrocyclic ligands, thus exploiting the chelate effect. Moreover, macrocyclic ligands could potentially be tuned to provide the best *fit* for specific cations and oxidation states by varying the size of the ligand's inner cavity, flexibility, etc.

In addition to the macrocyclic *fit/misfit* interactions, the choice of donor atoms might be another tool in the rational design of actinide separation or sequestering ligands. It is well-known that actinides form somewhat more covalent bonds than lanthanides and therefore have slightly better affinities for *soft* bases such as N-donor ligands. This could potentially be exploited in the separation of actinide cations from the lanthanides. So far, much of the attention has focused on comparisons between actinides and lanthanides in the oxidation state of III. Experimental data on the comparative covalency of $An(III)$ vs $Ln(III)$ were recently reviewed by Chopin.¹ Ionova² discussed the similarities and differences between $An(III)$ and $Ln(III)$ and pointed out that similarities do exist between the second half of the actinide series and the first half of the lanthanide series. However, relatively few studies, both experimental and theoretical, have been made on the degree of covalency of the equatorial bonding of the actinyl cations.

There are many types of macrocyclic ligands known to date. One family of ligands are porphyrins and phthalocyanins. The capacity of porphyrin and phthalocyanin to form stable aromatic complexes with transition metals is well-known. However, 1:1 in-cavity complexes between porphyrin and f-elements are unknown. Only actinide(IV) complexes of this ligand were obtained, which have the sandwich or 2:1 “double-decker” type, with the actinide atom residing above the porphyrin ligand plane.

* Corresponding author. E-mail: schrecke@cc.umanitoba.ca.

CHART 1: Alaskaphyrin 1, Bi-py-en 2 and Bi-pytmpd 3, Neutral H-forms

These findings are usually rationalized as *misfit* of a cation with the inner cavity of a porphyrin ligand that is regarded as being too small.

During the past decade, Sessler and co-workers have developed a new class of N-donor pyrrol-based macrocycles, called expanded porphyrins.³ They were able to obtain in-cavity 1:1 uranyl(VI)⁴ and neptunyl(V) and plutonyl(V)⁵ complexes for many of these ligands. It was shown⁵ that, for the neptunium and plutonium species, actinyl(V) complexes form, even when the actinyl oxidation state in the starting material was (VI).

Closely related to expanded porphyrins (but not strictly conforming to the definition of the expanded porphyrins because they contain only two pyrrolic groups), the macrocyclic Schiff-base ligand alaskaphyrin⁶ **1** (Chart 1) was developed and tested as an actinyl complexing agent. The uranyl complex of alaskaphyrin can be made either via ligand exchange or via template synthesis of alaskaphyrin around the uranyl cation. Complexes of neptunium(V) and plutonium(V) were obtained⁵ using the free ligand **1**.

The alaskaphyrin uranyl complex was the most celebrated because it is planar according to X-ray data. This could be seen as evidence of optimal “*fit*” or covalent bonding (supposing that covalent bonds are directed, compared to undirected ionic bonds, and therefore, in our case, would require an arrangement of the ligand donor atoms in the equatorial plane of the uranyl).

To determine whether the planarity is due to internal requirements of the uranyl cation or due to the rigidity of the phenylenediamine rings of the ligand, uranyl complexes of the alaskaphyrin analogues 3,6,13,16,21-hexaazapentacyclo[16.2.1.1^{8,11}.0^{4,5}.0^{14,15}]docosa-2,4,6,8,10,12,16,18,20-octaene (bi-py-en, **2**) and 3,7,13,18,23,24-hexaazapentacyclo[18.2.1.1^{9,12}.0^{4,5}.0^{15,16}]tetracos-2,7,9,11,13,18,20,22-octaene (bi-tpmd, **3**) ligands⁷ (see the structural formulas in Chart 1) were synthesized by Sessler’s group using template synthesis. It was found that the complexes formed by these ligands possess distorted geometries with a twist-like conformation of the ligand macrocycle; however, the

N-donor atoms form an almost planar arrangement in the equatorial plane of the uranyl cation.

The same ligands **2** and **3** can be obtained as free ligands without templating metal cations,⁸ which opens new possibilities for even more interesting experimental ligand exchange studies to form actinyl complexes of these ligands.

The article⁷ contains some data on the stability of the uranyl complexes of **1–3**, based on demetalation by acetic acid. An(VI)/An(V) reduction potentials (in CH₂Cl₂ solution) were measured as well. The availability of such data makes these complexes a valuable test system for the evaluation of theoretical methods.

Theoretical studies on the factors determining the stability of complexes between actinyls and expanded porphyrins could help in the development of new, more efficient systems. However, theoretical studies on expanded porphyrins and related Schiff bases themselves as well as their f-element complexes are still rather rare. There are various complications arising due to size of these systems, the importance of correlation and, for the actinide-containing systems, relativistic effects. Moreover, because many f-element complexes are ionic compounds, and very often processes under study happen in solution, it is not always easy to select a tangible model system. For these reasons, density functional theory (DFT) is the only practical approach.^{9,10} Recently, serious efforts have been made in improving computational DFT techniques (see, for instance, ref 11) as well as in developing reliable yet affordable relativistic methods.^{12–16}

As was noted above, the most obvious factors influencing the metal-to-ligand bonding are the nature of the ligand donor atoms and the shape and flexibility of the macrocyclic ligand. Clavaguera-Sarrio et al.¹⁷ performed a theoretical study on uranium(VI) complexes of the type UO₂L₂ with a variety of small monodentate ligands L, which included both *soft*- and *hard*-donor atoms. It was shown that the behavior of uranium(VI) is somewhat ambivalent. On one hand, the ammonia ligand binds slightly stronger than water, and phosphine stronger than H₂S. This can be interpreted as evidence of some “softness” of uranyl. On the other hand, a tendency of preference of the smallest donor atoms was found (F[−] over other halide anions, water over H₂S), indicating predominantly ionic bonding. The computational decomposition of the complex formation energy performed in that work showed, in addition to ionic interactions between ligands and the uranyl cation, some relevance of charge-transfer and polarization effects.

In the literature there are few theoretical studies on f-element complexes of Schiff-base ligands. Complexation of lanthanide cations with texaphyrin was studied using LC-ECPs (large-core effective core potentials) in reference.¹⁸ Brynda et al.¹⁹ have studied uranyl complexes of open-chain Schiff-base polydentate ligands using the ZORA (zeroth-order regular approximation) and SC-ECP (small-core ECP) relativistic approaches. They have found that the conformation of the salophene ligand is nonplanar in its uranyl complex due to Schiff-base nitrogen “puckering”—despite a conjugate π -system of aromatic rings and imine double bonds. This was explained by steric factors (the uranyl radius is too big for the ligand.)

Some theoretical calculations using DFT-GGA (generalized gradient approximation) methods were performed on 2:1 transition metal complexes of **1** (and **2**).²⁰ Not much detail is given, except that the complexes were apparently found to be planar.

The only theoretical paper on alaskaphyrin actinyl complexes published to date is an article by Kar and Liao.²¹ Alaskaphyrin complexes of uranium, neptunium and plutonium(VI) were

studied using DFT-GGA methods along with the quasi-relativistic Pauli Hamiltonian.^{22–24} They assumed the alaskaphyrin ligand and its actinyl(VI) complexes to be of D_{2h} symmetry. Binding energies from both neutral AnO_2 and neutral diradical alaskaphyrin fragments, as well from the corresponding dications and dianions were calculated as a measure of the affinities. The binding energies calculated from neutral fragments decrease along the series $\text{U} > \text{Np} > \text{Pu}$. The corresponding values for ionic fragments were found to be quite similar for all the actinyls ($\text{U}=\text{Np} = 28.05$ eV; $\text{Pu} = 28.14$ eV). Charge transfer from neutral AnO_2 to the neutral ligand was reported to be about $1 e^-$ (Mulliken charges) and the authors concluded that the actinyl–ligand bonding is “strong and covalent”. Ionization potentials and vertical electron affinities were calculated for the complexes; for U, unlike Np and Pu, the extra electron was found not in the metal f-orbital but in an orbital of the ligand π -system.

The present work has the following goals. (1) We will test the performance of existing DFT and relativistic effects methods using the available experimental data for the uranyl complexes of alaskaphyrin and related Schiff-base macrocycles. (2) We will investigate the ligand requirements, both sterical and electronic, for achieving the strongest possible complexation with the actinyl complexes. (3) We will explore periodic trends for the corresponding complexes of uranyl, neptunyl and plutonyl. For most of the calculations, model unsubstituted ligands were chosen for alaskaphyrin **1**, bi-pyen **2** and bi-tpmd **3** instead of the experimentally studied, tetraalkyl-substituted systems. We also considered tetramethoxy and tetranitro derivatives for the alaskaphyrin **1** uranyl complexes to determine the effects of ligand electronic factors. For neptunium and plutonium, only complexes of the unsubstituted ligands **1** and **2** were considered.

Details of the Calculations

Unless otherwise noted, full, unconstrained geometry optimizations were performed using the Priroda program.^{16,25,26} The code employs a fast resolution-of-identity method for calculating both Coulomb and exchange–correlation integrals with optimized fitting Gaussian basis sets. Priroda also applies a scalar four-component relativistic method where all spin–orbit terms are separated from scalar terms²⁷ and are neglected. All calculations with Priroda were done with the GGA PBE XC functional²⁸ and one of the two all-electron Gaussian basis sets: one of double- ζ -plus-polarization quality (AE-DZP) and another of triple- ζ plus polarization quality (AE-TZP) for the large component, and the corresponding kinetically balanced basis sets for the small component. Because the AE-TZP basis set was not yet available for either Np or Pu at the time of production of this work, we have used DZP basis sets for the AnO_2^{n+} species and their complexes, to have a consistent method for all three elements; for the uranium complexes AE-TZP basis sets were used except as otherwise noted. It should be noted that, for uranium complexes, both DZP and TZP bases yield very similar results for geometries, formation energies and the vibrational frequencies. After the major part of this work was done, a new family of optimized correlation-consistent basis sets of DZP, TZP and QZP quality became available for the Priroda code;²⁹ we used it to study basis set effects on the energies (see text and the Supporting Information).

Harmonic vibrational frequencies were calculated with the same program and basis sets to verify the nature of the stationary points obtained. They were also used for the thermochemistry. Throughout all the AE-TZP and AE-DZP calculations, strict

optimization and numerical integration criteria were applied (maximum component of the energy gradient to be less than 1×10^{-5} , grid accuracy parameter 1×10^{-8} , correspondingly).

The performance of relativistic AE-DFT calculations with the Priroda code as applied to the simulation of actinide molecules has not yet been evaluated in the literature in much detail. Hence, we have performed various test calculations on small molecules such as actinyl cations, actinide fluorides, oxides and oxofluorides. In all cases, we found Priroda to be entirely reliable in that it gives essentially the same results as other codes (and thus other relativistic methods), provided the same XC functional was used. We intend to publish a critical evaluation of different methods as applied to actinide molecules in a separate paper.³⁰ In addition, we have performed a throughout comparison of Priroda PBE results for hydration energies and redox potential of actinyls with SC-ECP and ZORA calculations which again showed that the code is entirely reliable.³¹

For the comparison of our GGA calculations with hybrid DFT methods for one case (alaskaphyrin uranyl complex), we also performed some geometry optimizations using the Gaussian03 program.³² In our Gaussian03 calculations, relativistic effects were included by replacing the core of the actinide element with a small-core ECP according to Küchle et al.¹⁵ We are thus treating 60 electrons as core, and the remainder as part of the variational valence space. Recently, it was shown that these “small-core” ECPs are much more reliable for the thermochemistry of uranium fluorides³³ than “large-core” ECPs (which replace 78 core electrons for an actinide atom). Likewise, “small-core” ECPs are superior to “large-core” ECPs in estimating both hydration energies and redox potentials of actinyl cations.³¹ We use the actinide basis sets that have been published for the SC-ECP by Küchle et al.¹⁵ but with the most diffuse s, p, d, f functions removed. The 6-31G all-electron basis sets implemented in Gaussian03 program package³² was used for carbon and hydrogen atoms; for the ligand atoms connected to the metal, oxygen and nitrogen, 6-311G(d) basis was used. All calculations were done with DFT in the form of either the well-established hybrid B3LYP^{34–36} or pure GGA PBE XC²⁸ functionals. So-called “fine” grids were used in all Gaussian03 DFT calculations for the sake of time economy, due to large size of calculated systems.

Finally, for the sake of properties, analysis and solvation methods available, some calculations were performed also with the scalar relativistic ZORA^{12–14} method as implemented in the Amsterdam density functional code ADF.^{37–39} ZORA is known to be of similar quality as the other relativistic methods employed in this study.^{30,31} The ADF-ZORA calculations we performed employed the following all-electron STO standard basis sets: ZORA-TZP for the uranium and donor atoms coordinated to it (O, N), ZORA-DZP for C and ZORA-DZ for H atoms of the macrocyclic ligand. The PBE XC functional was used.²⁸ A geometry optimization was performed for the alaskaphyrin case. For all the ADF calculations, an integration parameter of 5.5 was employed.

For some systems, we did ETS (Morokuma–Ziegler) energy decomposition analysis^{40–43} for the formation energy between UO_2^{2+} and a ligand dianion using single-point calculations with the ADF program based on the AE-TZP-optimized geometry. As is shown below for the example of the UO_2^{*1} complex, reoptimization with ADF does not lead to substantial changes in energies.

TABLE 1: Free AnO₂ⁿ⁺ Species, n = 1, 2, Geometries, AnO₂(VI)/AnO₂(V) Reduction Energies, Hirshfeld Charges and Spin Densities on Selected Atoms, and Actinyl Stretching Vibrational Frequencies (PBE, AE-DZP and AE-TZP Methods)

method	complex	$R_{An=O}$, Å	$\Delta G(VI-V)$, kcal/mol	$q(An)$	$q(O)$	spin on An	$\nu_{symm}(AnO_2)$	$\nu_{asymm}(AnO_2)$
AE-TZP	U ^{VI} O ₂ ²⁺	1.726		2.112	-0.056	0.0	997	1099
	U ^V O ₂ ⁺	1.781	-344.7	1.525	-0.263	1.069	911	987
AE-DZP	U ^{VI} O ₂ ²⁺	1.724		2.117	-0.058	0.0	965	1060
	U ^V O ₂ ⁺	1.777	-346.9	1.455	-0.227	1.087	896	969
	Np ^{VI} O ₂ ²⁺	1.723		1.990	0.047	1.098	934	1044
	Np ^V O ₂ ⁺	1.757	-361.6	1.420	-0.210	2.012	883	973
	Pu ^{VI} O ₂ ²⁺	1.713		1.923	0.038	2.212	901	1030
	Pu ^V O ₂ ⁺	1.743	-373.8	1.378	-0.187	3.326	875	969

In the calculation of the reduction potentials of the uranyl complexes of alaskaphyrin, bi-pyen and bi-tpmd, free energies of solvation were calculated by the COSMO^{44,45} continuum solvation model as implemented in the ADF code. Single-point ADF-COSMO calculations using the basis sets, density functional, and scalar ZORA relativistic method described above, were performed on AE-TZP optimized geometries. Klamt radii⁴⁶ were used for main-group atoms; the iron and uranium radii were taken as 1.50 and 1.70 Å, respectively. To model the dichloromethane solvent used in the experimental work, the dielectric constant of the solvent was set to 9.1.

All the calculations for systems with unpaired electrons were performed using the unrestricted Kohn-Sham formalism.

Results and Discussion

Geometries of Actinyl Sources. Bare actinyl species have been studied extensively by various theoretical methods.⁴⁷⁻⁵⁴ A detailed discussion of actinyls themselves is beyond the scope of the current paper. There are many excellent works on the electronic structure and bonding in actinyls.^{47,55,56} We will use bare actinyls only as reference points for calculating the complex formation energies and for charge comparisons. The structures, charge and spin density distribution, energies and vibrational frequencies of the bare actinyl species AnO₂ⁿ⁺ calculated by a variety of methods in our earlier work³¹ are summarized in Table 1.

As another reference point (see below in the discussion on energetics) for studying stabilities of complexes, uranyl(VI) and -(V) dichlorides were selected. Previously, uranyl(VI) dichloride was calculated by Kovacs and Konings,⁵⁷ and also by Clavaguera-Sarrio et al.¹⁷ in their comprehensive study on UO₂L₂ complexes. The geometry of this molecule, optimized with AE-TZP, was the following. The molecule has C_{2v} symmetry, with U=O and U-Cl distances of 1.794 and 2.599 Å correspondingly, and an O=U=O angle of 161.4°. The Cl-U-Cl angle has a value of 101.8°. This agrees with the results of the earlier calculations.

To our knowledge, no previous calculations were made on U^VO₂Cl₂⁻. The AE-TZP method gives a C_{2v} geometry with the U=O and U-Cl distances as 1.854 and 2.676 Å. The uranyl fragment is more distorted from linearity than for the U(VI) complex, with an O=U=O bond angle of 150.0°. The Cl-U-Cl angle is 112.4°. Thus, the geometry of uranium(V) dioxodichloride is shifted toward a tetrahedral configuration as compared to U^{VI}O₂Cl₂. The gas-phase free energy of reduction of the latter is found to be 60.9 kcal/mol.

Geometries of the Free Neutral Ligands 1-3 and Their Anionic Forms. To our knowledge, there are no experimental structural data available for the free-base and anionic forms of ligands 1-3. We found the free alaskaphyrin ligand H₂1 to be nonplanar, of C_{2v} symmetry, with the Schiff nitrogen atoms bending out-of plane (Figure 1). The distance between the

pyrrolic hydrogens is as big as 2.933 Å. Thus, the nonplanarity of the free base cannot be ascribed to the repulsion between these hydrogens. The dianion of alaskaphyrin is even more bent, obviously because of repulsion of the negative charges on the pyrrole groups. The tetramethoxy-, tetraethyl-tetramethoxy- and tetranitro-derivatives **1a**, **1b**, and **1c** are nonplanar in their neutral as well as dianionic forms.

For ligand **2**, there are (at least) two conformations possible: twist and chair (Figures 2 and 3, respectively). The neutral chair and twist forms have almost the same energy (the twist is less stable by only 0.3 kcal/mol). For the anionic forms, however,

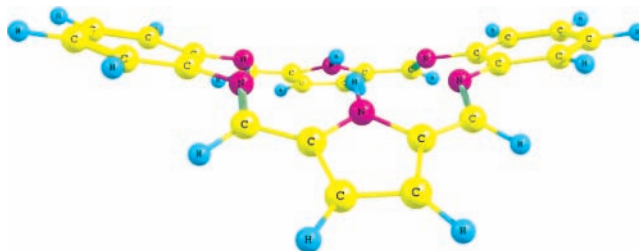


Figure 1. Alaskaphyrin **1**, free base form, AE-TZP geometry.

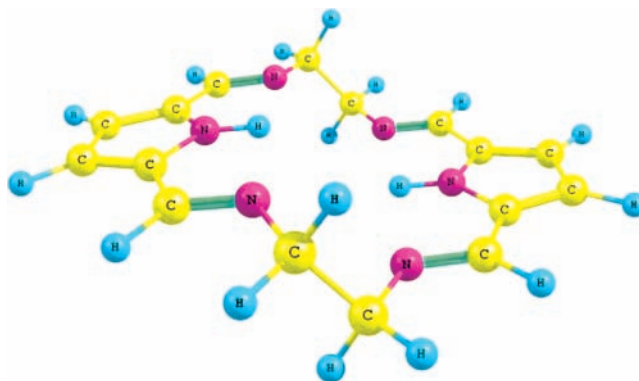


Figure 2. bi-pyen **2**, chair conformation, AE-TZP geometry.

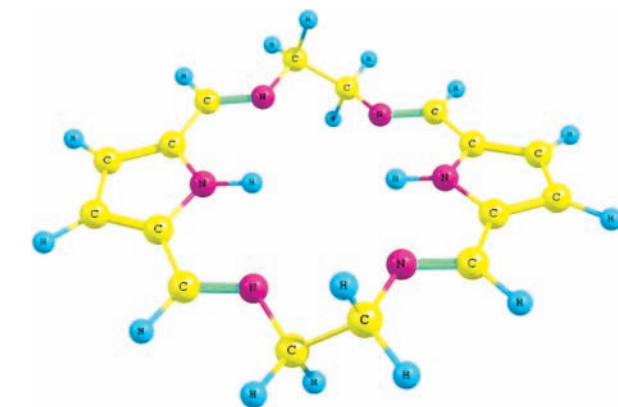


Figure 3. bi-pyen **2**, twist conformation, AE-TZP geometry.

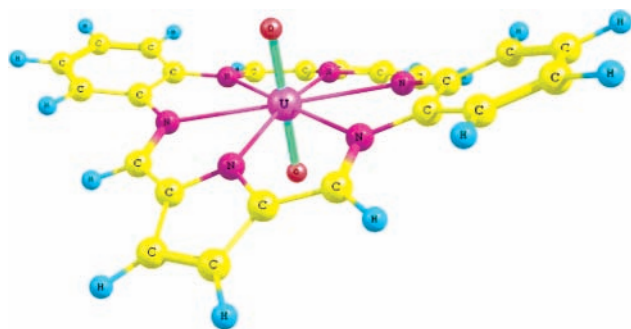


Figure 4. Alaskaphyrin complex $\text{UO}_2\mathbf{1}$, AE-TZP geometry.

the chair is 4.66 kcal/mol more favorable, again because of the same-charge repulsion. Ligand **3** is chemically similar to **2**; thus we considered only its twist-conformer.

Geometry of the Alaskaphyrin Uranyl(VI) Complex and Comparison of Theoretical Methods. According to the X-ray data available,⁶ the complex of alaskaphyrin with uranyl is planar. This makes it unique among the other expanded porphyrin complexes. For that reason, earlier calculations on it have been done assuming D_{2h} symmetry.²¹ Here, we performed an unconstrained geometry optimization of the $\text{UO}_2\mathbf{1}$ complex using AE-TZP, which lead to a saddle-type distorted structure (Figure 4). We also performed optimization for the complex imposing constraints on torsion angles around the imine $\text{C}=\text{N}$ bonds to keep it planar. The planar structure for the complex obtained is 2.88 kcal/mol less stable and has two small negative Hessian eigenvalues (second-order saddle point).

Inclusion of the methoxy and alkyl substituents to the model system does not lead to any significant conformation changes—complexes $\text{UO}_2\mathbf{1a}$ and $\text{UO}_2\mathbf{1b}$, $\text{UO}_2\mathbf{1c}$ are as nonplanar as $\text{UO}_2\mathbf{1}$.

To test the influence of the approximate relativistic method used in the calculations, we have performed geometry optimizations of the $\text{UO}_2\mathbf{1}$ complex with the ADF-ZORA and SC-ECP methods. For the latter, we have used not only the pure GGA density functional PBE but also the hybrid functional B3LYP. It has been shown³¹ that pure GGA functionals tend to slightly underbind the equatorial ligands in actinyl complexes as compared to experiment, whereas hybrid functionals perform better. Therefore, if the nonplanarity of $\text{UO}_2\mathbf{1}$ is an artifact of the PBE functional, then hybrid functionals should correct it.

Results of the calculations—key geometry parameters, uranyl vibrational frequencies and the energy differences between fully optimized, nonplanar complexes and planarized ones—are provided in Table 2. For the SC-ECP calculations (using both PBE and B3LYP), the minimum is again the bent structure, whereas the planar structures are again second-order saddle points. An unconstrained ADF-ZORA geometry optimization also leads to a bent structure very similar to the AE-TZP one. We did not determine the nature of the latter stationary point because of the high computational cost of numerical frequency calculations in ADF.

The geometries obtained by these methods can be compared to the experimental ones, Table 2. One can see that the PBE method systematically overestimates both the uranyl $\text{U}=\text{O}$ (to about 0.03 Å) and equatorial bond lengths for $\text{U}-\text{N}_1$ (pyrrolic nitrogen; see Chart 2). (For any approximate relativistic method used, the PBE geometries are very close.) Because the experimental configuration of the complex is planar, it is better to compare the experimental $\text{U}-\text{N}_2$ (Schiff-base nitrogen) distances against calculated planar structures. If so, there is a difference of 0.05–0.06 Å for any $\text{U}-\text{N}$ bond. The SC-ECP–B3LYP calculation yields $\text{U}=\text{O}$ distances within the error bar

of experiment, but the equatorial $\text{U}-\text{N}$ bond lengths given by this method are even longer than those given by PBE.

Interestingly, going from the free anion **1** to its uranyl(VI) complex, the Schiff $\text{N}_2=\text{C}_2$ bond length (numeration in Scheme 2) increases from 1.293 to 1.310 Å, whereas the C_1-C_2 bond shortens from 1.441 to 1.417 Å. The same bond length changes (relative to the “normal” single and double bond length values) were noticed in the original experimental work based on the X-ray geometry. This would lead to a somewhat greater degree of π -delocalization across the ligand circle.

Adding the electron donating methoxy groups to the phenyl rings of alaskaphyrin leads to a slight increase of both $\text{U}-\text{N}$ and $\text{U}-\text{O}$ distances, whereas acceptor nitro groups slightly decrease the distances between pyrrolic nitrogens and the uranium atom. There is a slight decrease of the uranyl stretching frequencies (see below) for complexes $\text{UO}_2\mathbf{1a}$ and $\text{UO}_2\mathbf{1b}$, and an increase for $\text{UO}_2\mathbf{1c}$, as compared to the nonsubstituted complex $\text{UO}_2\mathbf{1}$. This can be due to the well-known effect of competition for bonding of equatorial ligands with actinyl oxygens; the ligand with the lowest electron-donating ability **1c** destabilizes the uranyl bond to a lesser extent, and vice versa.

Geometries of the Bi-pyen and Bi-tpmd Uranyl(VI) Complexes. For the complexes of $\text{UO}_2\mathbf{2}$, as well as for its free ligand, there are two possible conformations, twist and chair. The twist conformer is slightly more stable (0.6 kcal/mol) than the chair conformer according to AE-TZP calculations. For the free ligand, the difference in stability between the conformers is very small (see above). The structure observed in the X-ray experiment is the twist conformer; so from now on, we will use only this one. For the bi-tpmd uranyl complex, we considered only the twist conformer, which again was observed by X-rays.⁷ Optimized geometries and uranyl stretching frequencies for these complexes are provided in Table 3. As in the case of the alaskaphyrin complex, PBE gives slightly longer uranyl and equatorial $\text{U}-\text{N}$ bonds than the experiment for both, $\text{UO}_2\mathbf{2}$ and $\text{UO}_2\mathbf{3}$. For the latter complex, one of the uranium to Schiff-base nitrogen bonds is elongated to 2.917 Å; it might be evidence that uranium prefers five- over six-coordination in the equatorial plane of the uranyl cation, which can be realized with the flexible-enough bi-tpmd ligand.

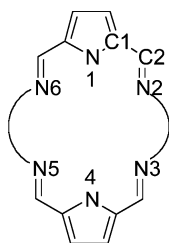
Both alkyl-diamino-based ligands give uranyl(VI) complexes with longer uranium to pyrrolic nitrogen distances than for the complexes of alaskaphyrin. For the complex of **2**, the distances between the metal atom and the four Schiff-base nitrogens are shorter than the corresponding distances in $\text{UO}_2\mathbf{1}$.

We notice that both the bi-pyen and bi-tpmd complexes of uranyl(VI) have a bent structure, with the nitrogen atoms distorted from the uranyl equatorial plane. Sessler et al.⁷ have used a dihedral angle between planar pyrrolic fragments of the ring (imine-pyrrolic-imine angle, calculated as the $\text{N}_2-\text{N}_1-\text{N}_4-\text{N}_6$ dihedral angle) as an index of the nonplanarity of the macrocyclic ligand ring. They found this angle to be about zero for $\text{UO}_2\mathbf{1}$, and 17.5° and 35.7° for $\text{UO}_2\mathbf{2}$ and $\text{UO}_2\mathbf{3}$, respectively. Our AE-TZP calculations show a slightly lower value for the bi-pyen complex, 12.4°. For bi-tpmd, there are two values (31.6° and 38.5°) because, as was mentioned above, the calculations yield a nonsymmetrical structure with one uranium–nitrogen bond elongated.

Geometry of the Alaskaphyrin, Bi-pyen and Bi-tpmd Uranyl(V) Complexes. The complexes of uranyl(V) with ligands **1–3** have a bent structure similar to those of the complexes of uranium(VI) described above. Despite the larger metal radius, as compared to that of uranium(VI), the alaskaphyrin complex of U(V) is still bent. The dihedral angles

TABLE 2: Optimized and Experimental Bond Lengths, Å, Relative Energies (See Text), kcal/mol, and Uranyl Vibrational Frequencies, cm^{-1} , for Calculated Planar and Nonplanar Alaskaphyrin 1 and 1a Dioxouranium(VI) Complexes

method	structure	$R_{\text{U=O}}$	$R_{\text{U-N1}}$	$R_{\text{U-N2}}$	$E - E(\text{planar})$	$\nu_{\text{symm}}(\text{U=O})$	$\nu_{\text{asymm}}(\text{U=O})$
AE-TZP, PBE, scalar four-component	planar $\text{U}^{\text{VI}}\text{O}_2\mathbf{1}$	1.801	2.457	2.771	0.0	841.5	929.7
	bent $\text{U}^{\text{VI}}\text{O}_2\mathbf{1}$	1.804	2.467	2.712	-2.88	834.5	922.2
ADF PBE, scalar ZORA	planar $\text{U}^{\text{VI}}\text{O}_2\mathbf{1}$	1.790	2.462	2.777	0.0		
	bent $\text{U}^{\text{VI}}\text{O}_2\mathbf{1}$	1.793	2.473	2.714	-4.29		
G03 PBE, SC RECPs	planar $\text{U}^{\text{VI}}\text{O}_2\mathbf{1}$	1.788	2.467	2.787	0.0	842.8	931.7
	bent $\text{U}^{\text{VI}}\text{O}_2\mathbf{1}$	1.792	2.474	2.716	-3.65	834.5	924.0
G03 B3LYP, SC RECPs	planar $\text{U}^{\text{VI}}\text{O}_2\mathbf{1}$	1.770	2.469	2.790	0.0	883.7	974.5
	bent $\text{U}^{\text{VI}}\text{O}_2\mathbf{1}$	1.773	2.477	2.734	-2.56	879.9	968.5; 971.0
AE-TZP, PBE, scalar four-component experiment ^a	bent $\text{U}^{\text{VI}}\text{O}_2\mathbf{1a}$	1.806	2.470; 2.468	2.717		828.7	917.9
	planar $\text{U}^{\text{VI}}\text{O}_2\mathbf{1a}$	1.770(6)	2.418(7)	2.733(7); 2.748(7)			910

^a Reference 6.**CHART 2: Numeration of the Ligand Atoms Used in This Work**

between the pyrrolic and imine nitrogens for the bi-pyren and bi-tpmd complexes become lower, but they are still quite far from zero (10.4° for $\text{UO}_2\mathbf{2}^-$, and 27.9° and 27.5° for $\text{UO}_2\mathbf{3}^-$).

The uranium–oxygen and uranium–nitrogen bonds of the uranyl(V) complexes are longer than for the corresponding uranium(VI) compounds, Table 2. Interestingly, although the calculated U=O bond lengths are similar for all the complexes of uranyl(VI), for uranium(V), there is an increase in bond lengths from **1** to **2** to **3**. This can be, rather speculatively, explained by a better degree of delocalization of the extra electron in the conjugated alaskaphyrin ligand π -system, and therefore lesser destabilization of uranyl. Equatorial uranium–nitrogen bond lengths are also longer for the complexes of U(V) than for U(VI); the distances between uranium and the pyrrolic nitrogens increase strongly when we go from uranium(VI) to uranium(V) complexes as **3** > **2** > **1**.

We observe the same change in C1–C2 and C2–N2 bond lengths for U(V) complexes as for U(VI) ones: Schiff-base C2=N2 bonds are elongating, whereas pyrrol to Schiff-base carbon C1–C2 bonds are shortening as compared to free ligand.

Charge Distribution and Bond Orders of the Alaskaphyrin, Bi-pyren and Bi-tpmd Uranyl(V,VI) Complexes. Liao et al.²¹ used Mulliken charges on the actinyl fragment to draw conclusions about the covalent character of the metal–ligand bonding. In this work we will look in more detail into the charges and bonding.

We have chosen Hirshfeld charges⁵⁸ to analyze the charge and spin density distribution in our complexes. Previously, it was shown⁵⁹ that these charges change reasonably with molecular structure changes. It should be noted that Hirshfeld charges are usually “smaller” than charges calculated by other methods. We also analyze the bonding in our uranyl complexes using Mayer’s population-based bond orders (see ref 60 and references herein). Previous experience shows that, despite their basis-set dependence, population bond orders are a useful tool in the coordination chemistry of d-elements.^{61,62} Recently, it

has been shown that these population-based bond orders provide reasonable results for actinide compounds.^{63,64}

In addition to complexes and free neutral ligands, ligand dianions were also calculated by us as one of the possible reference points for estimating the complex stabilities. It shall be noted that the GGA-DFT has some trouble describing anions in general: although the exact Kohn–Sham DFT is supposed to work well, all approximate functionals are known to give nonbound states for the anions (provided that a complete basis set is used). For dianions, obviously this situation would be even worse. However, it must be said that in practical calculations using finite basis sets the DFT deficiency is somewhat canceled. It was found⁶⁵ that PBE is a rather good functional with only moderate errors for electron affinities. Moreover, the errors seem to be smaller for bigger systems. We decided to calculate the dianions of our ligands despite the mentioned problems; the performance of our method is discussed below. Selected results for partial atomic charges in the species and bond orders in the complexes are provided in Table 4.

The dianions of the Schiff-base macrocycles, especially those based on aliphatic diamines (ligands **2** and **3**), do not delocalize the negative charge very effectively; the charge is mostly localized on the pyrrolic nitrogens. It is not surprising that, in complexes of uranyl(VI), the charge on the ligand donor atoms decreases as compared to the free ligand dianions. The pyrrolic nitrogens in these complexes still bear more negative charge than the Schiff-base ones. Charges on the latter in the free ligands, anion forms and complexes are closer to each other than the charges on pyrrolic nitrgens that change strongly. The sum of the Hirshfeld charges on the uranyl(VI) fragment is close to zero (about 0.01–0.03). This indicates that there is significant charge transfer due to polarization of the ligand dianion by the uranyl dication; this was also noticed by Liao et al.²¹ Taking into account the character of the charge changes on nitrogens, mentioned above, we can conclude that charge transfer happens mostly between pyrroles and uranyl, and less between Schiff-base nitrogens. Comparing the charges on the uranium and oxygen atoms with the ones in free uranyl, provided in Table 1, one can see that the uranyl oxygens in the complex bear a larger negative charge and, even though the uranyl fragment has a total charge of about zero, the metal atom still bears some positive charge.

Introduction of the electron-donor methoxy or electron-withdrawing nitro substituents into the alaskaphyrin phenyl rings changes the partial charges on the ligand donor atoms accordingly: For the tetranitro-derivate **1c**, there is a decrease of partial negative charges on the ligand donor atoms as compared to

TABLE 3: Optimized (AE-TZP) and Experimental Bond Lengths, Å, and Uranyl Vibrational Frequencies, cm⁻¹, for Calculated Dioxouranium(VI) and -(V) Complexes and Their Experimental Analogs, Where Available

complex		U=O	U–N1	U–N2	U–N3	U–N4	U–N5/O1	U–N6	ν_{symm}	ν_{asymm}
U ^{VI} O ₂ 1	calc	1.804	2.467	2.712	2.712	2.467	2.712	2.712	834.5	922.2
	expt ^a	1.770(6)	2.418(7)	2.733(7)	2.733(7)	2.418(7)	2.740(5)	2.740(5)		910
U ^{VI} O ₂ 1b	calc	1.804	2.468	2.721	2.719	2.468	2.721	2.719	833	923
U ^{VI} O ₂ 1c	calc	1.800	2.464	2.722	2.715	2.464	2.723	2.714	843	929
U ^{VI} O ₂ 2	calc	1.807	2.483	2.696	2.696	2.483	2.696	2.696	830.8	916.1
	expt ^b	1.774(3)	2.456(3)	2.6608	2.6569	2.456(3)	2.656(3)	2.6521		897
U ^{VI} O ₂ 3	calc	1.804	2.473	2.731	2.917	2.481	2.740	2.725	828.5	916.0
	expt ^b	1.777(2)	2.444(3)				2.660(2)			897
U ^V O ₂ 1 ⁻	calc	1.817	2.481	2.729	2.762	2.481	2.729	2.762	781.0	895.6
U ^V O ₂ 2 ⁻	calc	1.837	2.513	2.713	2.723	2.509	2.723	2.696	750.8	858.3
U ^V O ₂ 3 ⁻	calc	1.842	2.540	2.819	3.042	2.541	2.800	2.840	736.8	851.1

^a Reference 6. ^b Reference 7.

TABLE 4: Hirshfeld Charges on Ligand Donor Atoms in Free Neutral and Anion and Complexed Ligand Forms and Uranyl Moiety, and Population-Based U–X Bond Orders, AE-TZP

complex	U charge	O		N1, N4		N2–N5, N6	
		charge	bond order	charge	bond order	charge	bond order
H ₂ 1				–0.018		–0.145	
1 ²⁻				–0.190		–0.143	
U ^{VI} O ₂ 1	0.638	–0.313	2.21	–0.126	0.55	–0.093	0.34
U ^{VI} O ₂ 1 ⁻	0.589	–0.349	2.16	–0.136	0.55	–0.108	0.35
H ₂ 1b				–0.046		–0.140	
1b ²⁻				–0.189		–0.142	
U ^{VI} O ₂ 1b	0.636	–0.314	2.20	–0.128	0.55	–0.094	0.34
H ₂ 1c				–0.043		–0.132	
1c ²⁻				–0.178		–0.128	
U ^{VI} O ₂ 1c	0.656	–0.303	2.21	–0.122	0.55	–0.091	0.33
H ₂ 2				–0.048		–0.136	
2 ²⁻				–0.189		–0.145	
U ^{VI} O ₂ 2	0.622	–0.319	2.19	–0.127	0.56	–0.091	0.36
U ^V O ₂ 2 ⁻	0.519	–0.379	2.12	–0.134	0.50	–0.106	0.36
H ₂ 3				–0.048		–0.138;	
						–0.147	
3 ²⁻				–0.200		–0.166;	
						–0.145	
U ^{VI} O ₂ 3	0.656	–0.314	2.19	–0.129	0.58	–0.089;	0.36;
						–0.090	0.26
U ^V O ₂ 3 ⁻	0.532	–0.391	2.09	–0.132	0.46	–0.097;	0.28;
						–0.116	0.22

unsubstituted ligand **1** in both the free anion form and the uranyl-(VI) complex, especially for the pyrrolic nitrogens. For the tetramethoxy-derivate **1b**, there is slightly more negative charge on the nitrogens in the uranyl complex.

When we go from uranium(VI) to uranium(V), there is a decrease of positive charge on the uranium atom, increase of negative charge on the uranyl oxygens, and increase of negative charges on the ligand nitrogens as compared to the uranyl(VI) complex. Interestingly, the differences are smaller for complexes of **1** than those of **2** and **3**. This can be explained in terms of a better ability of the conjugated cyclical π -system of **1** to delocalize the extra electron. (See also the respective discussion of bond lengths above.)

It should be noted that the definitions of “ionic” and “covalent” bonds for a coordination compound are necessarily qualitative. Although there are some pure (i.e., nonpolar) covalent bonds known, a pure “ionic” situation is not. This is because there is always some amount of polarization of the anion by the cation in the ionic bond, which leads to some covalent character (and thus a nonzero bond order).

In this connection, we need to mention one other issue. In coordination compounds, all the metal-to-ligand coordination bonds are always delocalized.⁶⁶ Therefore, speaking of a bond

property between the metal and a ligand always refers to “the bond between the metal and the ligand within a given ligand environment” or, in other words, a bond property between the metal and all the ligands around it. This is a very general fact, and actinyls, despite being very stable moieties, are no exception: One can see that actinide-oxygen bond lengths, bond orders and vibrational frequencies indeed do change significantly with varying equatorial ligands (see Table 3).

Although there is no established quantitative index of covalency for coordination bonds (at least to our knowledge), the concept of “degree of covalency in a complex” is still useful (and has been widely discussed, with respect to spectroscopy, see, e.g., ref 66). Here, we will try to employ population-based bond orders as such an index. Though basis set dependent, population based bond orders can be used for a qualitative description of the bonding in the complexes, in the sense that they show the amount of density “between bonded atoms” which can be crudely linked to the degree of ionicity/covalency of the corresponding bond: the stronger the polarization, the more covalent the character of the bond would be, and a correspondingly higher population bond order would have to be expected.

An example for an actinyl complex that is nearly “ionic” in that sense might be the complex of 18-crown-6 (a neutral aliphatic ligand with “hard” donor atoms, ether oxygens, without anything as easily polarizable as for example a π -system) with uranyl(VI), which has U–O(eq) bond orders of 0.33 (ref 67 calculated with the same AE-TZP method as applied in the present work).

Population-based uranyl bond orders (Table 4) show that uranyl bonds have a bond order higher than 2, in good agreement with the generally accepted view that these bonds possess partial triple bond character. Reduction of the uranyl(VI) to -(V) decreases the corresponding bond orders because the extra electron should go to a nonbonding f-orbital of the metal, although there is still some triple bond character left.

Bond orders for bonds between uranium and the equatorial ligands are substantially less than 1, with higher orders for the pyrrolic nitrogens than for the Schiff-base ones. Together with the charge distribution (see above), this can be interpreted as an evidence of an essentially ionic character of the equatorial uranium to Schiff nitrogen bonds in our complexes. (Uranium to pyrrolic nitrogen bonds having higher bond orders are to be treated as “more covalent”.) The values of the bond orders between uranium and the Schiff-base nitrogens (0.34–0.36, Table 3) are very close to the ones for the “noncovalent” 18-crown-6 complex mentioned above, suggesting the view that these bonds can be described as “ionic”.

The equatorial bond orders change differently upon uranyl reduction for the complexes of alaskaphyrin **1** and bi-pyren, bi-tpmd **2** and **3**: Although for the former there is no substantial

TABLE 5: Dioxouranium(VI) and -(V) and Ligand Anion Formation Energies and Its Morokuma/ETS Decomposition, kcal/mol, AE-TZP(Priroda) and ADF-ZORA, PBE^a

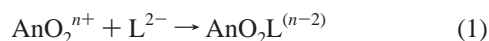
complex	$E(2)$	$E_{\text{ligand}}^{\text{def}}$	$E_{\text{UO}_2}^{\text{def}}$	E_{prep}	E_{int}	$E_{\text{int}}(\text{ADF})$	E_{Pauli}	E_{Elstat}	E_{Orb}	$\Delta H_{298}(4)$
$\text{U}^{\text{VI}}\text{O}_2\mathbf{1}$	-638.7	17.7	7.1	24.8	-663.4	-662.5	182.7	-553.8	-291.4	-28.1
$\text{U}^{\text{VI}}\text{O}_2\mathbf{1}(\text{ADF})$	-635.8	19.7	6.6	26.3	-662.0	-659.5	180.9	-551.3	-289.1	
planar $\text{U}^{\text{VI}}\text{O}_2\mathbf{1}$	-633.4	20.3	6.2	26.5	-659.8	-660.2	173.5	-554.7	-279.0	
planar $\text{U}^{\text{VI}}\text{O}_2\mathbf{1}(\text{ADF})$	-629.1	23.2	5.7	28.9	-658.0	-657.6	171.2	-552.8	-276.1	
$\text{U}^{\text{VI}}\text{O}_2\mathbf{1b}$	-634.6	23.2	5.7	28.9	-657.9	-668.3	180.5	-555.7	-293.1	-28.4
$\text{U}^{\text{VI}}\text{O}_2\mathbf{1c}$	-575.9	16.9	6.5	23.5	-599.3	-602.7	180.4	-486.9	-296.2	-25.4
$\text{U}^{\text{VI}}\text{O}_2\mathbf{2}$	-668.6	12.6	7.6	20.1	-688.7	-693.8	184.4	-587.8	-290.3	-33.2
$\text{U}^{\text{VI}}\text{O}_2\mathbf{3}$	-642.2	23.5	7.2	30.7	-672.9	-678.7	176.7	-576.8	-278.5	-20.9
$\text{U}^{\text{V}}\text{O}_2\mathbf{1}$	-335.7	17.2	1.5	18.7	-354.4	-379.0	171.5	-376.2	-174.4	-13.3
$\text{U}^{\text{V}}\text{O}_2\mathbf{2}$	-351.8	10.9	3.3	14.2	-365.9	-368.6	168.5	-357.0	-180.1	-4.9
$\text{U}^{\text{V}}\text{O}_2\mathbf{3}$	-327.6	14.7	3.8	18.6	-346.1	-350.8	139.6	-350.7	-139.7	5.4

^a See text for details.

change, for the two latter there is a significant decrease in the bond orders of the (pyrrolic) U–N1 and U–N4 bonds for **2**. Likewise, all U–N bond orders decrease for **3**. The reason for this could be the different flexibility of the ligands—the more flexible the ligand is, the easier it adapts to the bigger uranyl-(V) cation by increasing the U–N distances, and the lower the population bond orders will become (because of a decrease in overlap for longer bonds.)

Energetics and ETS Analysis for the U(V) and U(VI) Complexes. Selection of a meaningful model is not an easy task for actinide coordination chemistry. The straightforward calculation of the free energy corresponding to the real ligand-exchange process is not possible due to problems arising from accounting for many possible reagents' and products' forms, as well as bulk solvation effects. Therefore, one has to choose a model that could adequately describe some key factors in the real process, but would be simple enough to deal with.

One of the simplest quantities to analyze is the complex formation energy between a central atom or group (in our case the actinyl ion) and the ligands. The Hirshfeld charges on uranium atom that are considerably positive, and the bond orders between uranium and nitrogen atoms well below unity show that the bonding in the alaskaphyrin, bi-pyen and bi-tpmd complexes, at least for Schiff-base nitrogens, can be described as ionic. Therefore, although the energy with respect to the neutral fragments radical in the gas phase will certainly be lower (ref 21 and see also Table S2 in the Supporting Information), for the modeling of complexes in solution the ionic dissociation (as in eq 1) is in our opinion more relevant. As was noted above,



however, that scheme leads to a problem with describing ligand dianions. DFT calculated anions give higher occupied molecular orbitals with positive energy; electrons are not leaving to continuum only because finite basis sets are employed. Therefore, the calculated energy of (1) might depend heavily on the basis set; and it is not clear whether the error associated with the anion energy is the same for the different ligands that we compare against each other. In the Supporting Information we evaluate this using the recently published correlation-consistent family of basis sets for the Priroda code.²⁹ In summary, although there indeed is some basis-set influence on the energies of (1), and the corresponding changes in the energy of (1) are bigger for ligand **2** than for **1**, the magnitude of the difference is of a few kcal/mol and never changes the qualitative picture of preference of ligand **2** over ligand **1**. We have also calculated energies for the formation of uranyl complexes of alaskaphyrin and bi-pyen from uranyl(IV) and free radical ligand fragments

(Table S2) and note that the same qualitative picture as for the ligand dianions is observed.

In any case, the energy of reaction 1 allows for an easy comparison between An(V) and -(VI) and can be analyzed further in terms of the interactions between actinyl and ligand fragments, so we calculated the corresponding values. Formation energies of the uranyl(VI) and -(V) complexes of alaskaphyrins, bi-pyen and bi-tpmd, defined as Eq(1), are summarized in Table 5.

The $\text{U}^{\text{VI}}\text{O}_2\mathbf{2}$ complex has the most negative formation energy. The complex of **3** has a somewhat higher formation energy that is, however, still more negative than that of the uranium(VI) complex of the unsubstituted alaskaphyrin **1**. For the uranium-(V) case, the complex of bi-pyen has again a significantly more negative formation energy than the complexes of either bi-tpmd **3** or alaskaphyrin **1**. (The latter is now more stable than the former, though.)

To further explore the bonding in these complexes, we employed an analysis of the ligand-to-uranyl formation energy using the ETS energy decomposition scheme.^{40–43} In this scheme, the dissociation energy of a molecule into some fragments [in our case, the energy of reaction 1 because we decided to use charged uranyl and ligand anion fragments] is separated into two components,

$$E(1) = \Delta E_{\text{prep}} + \Delta E_{\text{int}} \quad (2)$$

Here ΔE_{prep} is the energy of promotion of the fragments from their equilibrium geometry to the geometry they will have in the complex (there will be no change in the electronic state in our case), and ΔE_{int} is the energy of interaction between the fragments in the complex. The latter term in the ETS scheme can be divided as

$$\Delta E_{\text{int}} = E_{\text{Pauli}} + E_{\text{Elstat}} + E_{\text{Orb}} \quad (3)$$

Here E_{Pauli} gives the energy of the four-electron Pauli repulsive interaction between occupied orbitals of the fragments and E_{Elstat} is the electrostatic interaction energy of the fragments that are calculated with a “frozen” electron density distribution. Finally, E_{Orb} is the rest, comprising the relaxation energy of the “frozen” orbitals into their final form in the complex. The latter term can be roughly identified with charge polarization and covalent interactions. The applicability of the ETS scheme to the main group donor–acceptor and transition metal complexes was recently reviewed and discussed by Frenking et al.⁶⁸ and Atanasov et al.⁶¹

The fragments can be selected as either neutral open shell dioxouranium(IV) and ligand diradical or cationic for uranyl

and dianionic fragment for the ligand. It was shown⁶¹ that for Werner-type complexes of the d-elements ionic fragments make more sense, whereas for organometallics neutral radical fragments can be more meaningful. Koenigs and Kovacs⁵⁷ argued that neutral fragments have to be employed for the UF₆ and UO₂F₂ cases. We, however, note that for these compounds bond orders are high (larger than unity).⁶⁷ Geometrical differences between bi-pyren, bi-tpmd and alaskaphyrin complexes are mainly related to uranium–Schiff-base nitrogen distances, and the corresponding bonds have small bond orders. Moreover, charges on the Schiff-base nitrogens do not change so much as on pyrrolic ones for neutral ligand, dianion and complex cases, so we believe that “polarization” of the fragment taken as ionic happens mostly on the latter. Thus we have chosen ionic L²⁻ and UO₂ⁿ⁺ fragments.

Results of the ETS fragment calculations for our complexes are summarized in Table 5. Because we have used AE-TZP calculations to optimize geometries, the ΔE_{prep} terms have been calculated with the AE-TZP method as well, i.e., as differences between the energies of optimized ions and their corresponding fragments calculated with AE-TZP. Then, ADF-ZORA PBE single-point fragment calculations were performed, and ΔE_{int} is a result of these ADF calculations.

First of all, we have to justify our scheme of using ADF fragment calculation on AE-TZP optimized geometries by comparing the results with fully ADF-optimized structures, using the example of both planar and bent UO₂**1** complexes. One can see that at least for the uranium(VI) complexes the differences introduced by re-optimization are not drastic, the trends in general remain the same, and the absolute values of ΔE_{int} as well as its components are pretty close for the results of both procedures, Table 5. (The only exception for that is the alaskaphyrin uranyl(V) complex, for which the total formation energy calculated by ADF differs from E_{int} as obtained by AE-TZP by more than 20 kcal/mol. This might be a result of some peculiarities of the ETS analysis procedure of the ADF code, which cannot presently handle unrestricted fragments. For that reason, the open-shell uranyl fragments were calculated in an averaged, closed-shell approximation. Then their occupations were modified to correspond to UHF solutions. There is no other way in ADF to perform ETS energy decompositions on open-shell complexes. However, because the “UHF” orbitals that were obtained in this manner are not self-consistent, this might lead to some amount of error.)

As one can see, the E_{Elstat} components are by far the most important contribution to the attractive interaction between the fragments for our decomposition scheme (i.e., ligand dianion and uranyl cation as fragments). The electrostatic energy gets significantly lower for the complexes of uranium(V) than for the ones of uranium(VI); E_{Orb} decreases as well (which reflects a lesser degree of ligand polarization inflicted by the less positively charged uranyl(V)) but the overall $E_{\text{Elstat}}/E_{\text{Orb}}$ ratio remains high. The prevalence of electrostatic term in the fragments interaction energy is indeed constructed by our initial selection of ionic fragments. However, for really covalent organometallic compounds (like ferrocene, for example) the contribution from E_{Orb} is substantially higher than that, even for ionic fragments.

The ETS analysis can be employed to understand the reasons for the nonplanarity of the alaskaphyrin complex. First, the deformation energy E_{Prep} for the bent and planar complexes is slightly (1.7 kcal/mol) less for the bent conformation than for the planar one. This should be expected because, as we have seen earlier, both the free alaskaphyrin ligand and its dianion

form prefer nonplanar C_{2v} configurations. However, not only the deformation energy favors this configuration of the complex but E_{int} does also. The differences in E_{int} between the planar and nonplanar form of the alaskaphyrin complexes are mainly due to E_{Orb} . The Pauli repulsion term is slightly more favorable for the planar structures, which is clearly due to its longer metal-to-nitrogen bonds. E_{Elstat} stays almost the same (actually, it is slightly more favorable for the planar one.) It seems that the nonplanarity, which allows for shorter U-to-Schiff-N bonds, thus favors polarization and covalent interactions.

Introducing electron-withdrawing nitro-groups to **1**, giving **1c**, leads to a drastic decrease of its affinity to uranyl, again due to a decrease in the absolute value of E_{Elstat} . (This result goes along with “chemical intuition”. Thus, it illustrates to some degree that the energy decomposition scheme we use is meaningful.) Tetra-methoxy substituted alaskaphyrin **1b** has a slightly more negative internal formation energy than the unsubstituted species **1** due to E_{Elstat} . However, the deformation energy E_{Prep} for it is higher as well, so there is no significant increase of the formation to the uranyl due to these substituents. The behavior of the electrostatic energy contribution E_{Elstat} for the uranyl complexes of **1**, **1b** and **1c** is in agreement with the values of the Hirshfeld charges for the corresponding free ligand anions (Table 4)—the more negative the charges are, the higher is the absolute value of E_{Elstat} .

As we mentioned above, ligands **2** and **3** have more exothermic complex formation energies $E(1)$ than alaskaphyrin **1**. The reason for this is mainly found in a more negative E_{Elstat} for the former two ligands. The atomic charges on the free bi-tpmd anion (Table 4) do not differ strongly, so the increase in the absolute value of the electrostatic energy for this ligand must result from shorter uranium to Schiff-base nitrogen bonds in the [UO₂]ⁿ⁻ complexes (Table 3).

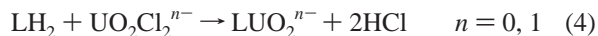
The differences between **2** and **3** can be rationalized as follows. The deformation energies E_{Prep} are optimal for the bi-pyren ligand **2**, considerably lower than for **3** (and slightly lower than for **1**.) As was mentioned above, the complex of the bi-tpmd ligand **3** has one of the six nitrogen donor atoms uncoordinated. This explains both the lower Pauli repulsion and the less negative orbital interaction terms for it, as compared to the complex of **2**. The electrostatic interaction energy of the uranyl(VI) complex of **3** could be lower than that of **2** (despite the more negative charges on the nitrogens of the free ligand anion of the former), in part at least, for the same reason—there are only five N-donor atoms coordinated.

One can see that for all the uranyl(VI) alaskaphyrin complexes **1**, **1b**, **1c**, the Pauli repulsion energy is almost the same, Table 5. The uranyl(VI) complexes of **2** and **3** have only slightly less E_{Pauli} than those of **1**. At the same time, for the complexes of uranyl(V), there is a strong decrease of E_{Pauli} in a row of **1** > **2** > **3**. This follows directly from the geometry changes discussed above.

Interestingly, the relative order of the E_{Elstat} absolute value changes, from **2** > **3** > **1** for U(VI) to **1** > **2** > **3** for U(V) complexes.

As was discussed above, there are some difficulties with calculating complex formation energies using reaction 1 due to the problematic treatment of dianions with DFT. In addition to that, there is another important factor, the acidity of neutral forms of the ligands. Highly unstable anions such as 2²⁻ and 3²⁻, which have very high affinities to the uranyls, may have higher affinities for the protons as well. Therefore, it is useful to also consider the process starting from the neutral ligand form and releasing ligand proton in some form. One of the possible

model gas-phase reactions is eq 4: uranyl dichloride is selected because it is one of the real sources of uranyl in the synthesis of expanded porphyrin complexes. (Of course, the choice of a uranyl-containing source for the relative comparison of ligands **1–3** can be arbitrary; any other uranyl complex could be taken without influencing the results.) Comparing affinities to the ligand of uranium(V) with uranium(VI) is not that straightforward as in the model eq 1. To achieve this comparison, we take an anion $\text{U}^{\text{V}}\text{O}_2\text{Cl}_2^-$ as the source compound.



Corresponding calculated reaction enthalpies are provided in the last column of Table 5. Differences between **1**, **2** and **3** are now much smaller than for reaction 1 as expected. For the uranium(VI) case, bi-tpmd is now less favorable than alaskaphyrin. This goes along with the speculation above about lower basic character of the ligand dianion for the latter. The bi-pyren complex is the most favorable one nonetheless. The energies of reaction 4 for methoxy- and nitro-substituted alaskaphyrins **1b** and **1c** vary similarly to the energies of eq 1: for the former it is slightly more negative, and for the latter less negative than for the unsubstituted ligand **1**; still, ligand **2** is more favorable than any of the **1** derivatives.

For the complexes of uranium(V) the trend of energies according to eq 4 is different: the most stable is the complex of alaskaphyrin, and the least the one of bi-tpmd.

Let us briefly summarize and conclude the preceding sections as follows. The ETS analysis, performed under the assumption of the ionic fragments, allows us to explain the differences in affinities according to the eq 1 between alaskaphyrin and bi-pyren, bi-tpmd ligands by better electrostatic interactions for the two latter. Because the interaction is not directional (as opposed to covalent one), puckering of the ligand donor atoms from the equatorial plane of the uranyl cation does not lead to significant losses in their bonding ability. The ligand affinity as defined by eq 1 is, indeed, not the only factor; this is shown by the calculations using eq 4. However, it will play some role if the other conditions are kept the same.

The most important conclusion is that there is no point in trying to design macrocyclic ligands forming planar complexes. Instead, an optimal ligand might have to be flexible enough to be able to provide the necessary deformations that result in optimal uranium to donor-atom distances (which for the case of coordination of five or six sp^2 -hybrid nitrogen donor atoms, are about 2.52 Å). Among the Schiff-base macrocyclic ligands, the bi-pyren ligand **2** has the strongest affinity to uranyl(VI), for the very reasons described above. Alaskaphyrin **1** is less favorable in comparison because of the rigidity of its phenylene rings.

Although we now understand the formation energy of the ligand anions to the uranyl cations, the connection of it to the experimentally observed kinetic and thermodynamic stabilities of the complexes is not that straightforward because many other factors might influence the latter. However, some conclusion can be drawn even from the data we have. Experimental data are available on the demetalation of the uranyl(VI) complexes of **1–3** by acetic acid.⁷ Although the first two are stable for up to 72 h, the last gets demetalated rather fast. Because the X-ray structures of the uranyl complexes of bi-pyren **2** and bi-tpmd **3** reported in that work appear to be very similar structurally, this difference needs an explanation.

It is widely accepted⁶⁹ that demetalation (i.e., substitution of the macrocyclic ligand by solvent molecules in the metallo-complex) proceeds via a mechanism that includes protonation

of a ligand nitrogen atom as a first step. For the octacoordinated uranium we have in our uranyl complexes of hexadentate ligands, the mechanism should be expected to be dissociative. The nonsymmetric, almost five-coordinated, structure of $\text{UO}_2\mathbf{3}$ predicted by our gas-phase calculations might allow this process to proceed more easily than the alaskaphyrin and bi-pyren uranyl complexes, where all six nitrogens are strongly bound to the uranium, and therefore nitrogen protonation in that case (which effectively requires breaking one of the N–U bonds) would require more energy, leading to a higher activation barrier of the process.

To test that hypothesis, proton affinities corresponding to protonation of either pyrrolic or Schiff nitrogen atom were calculated for the uranyl(VI) complexes of **1–3**. Structures of the Schiff-base protonated form of $\text{UO}_2\mathbf{3}$ are provided in Figure 8. In the case of protonation of a pyrrolic nitrogen, calculated proton affinities were very close for all three complexes, –228.5, –227.1, and –228.2 kcal/mol correspondingly. Relative stability of the Schiff-base nitrogen-protonated product with respect to the pyrrolic-protonated one differs. For the alaskaphyrin complex, it is 4.4 kcal/mol less stable, whereas for bi-pyren, it is 4.3 kcal/mol more stable. Finally, for the bi-tpmd uranyl complex, the Schiff-base protonation product lies 9.3 kcal/mol below the pyrrolic one, which means significantly easier protonation than for complexes of **1** and **2**.

Neptunium and Plutonium Complexes. Calculations for the neptunium and plutonium complexes of alaskaphyrin **1** and bi-pyren **2** were performed with the DZP basis sets available for these elements in the Priroda program; for compatibility, uranium complexes were recalculated using the same basis. There is no significant loss of quality as compared to the (older) TZP basis, because the DZP basis sets are highly optimized.

With these settings, we have investigated the geometries, formation energies according to eq 1, bond orders, charge and spin distributions for all the AnO_2^{n+} complexes of **1** and **2**. Moreover, we have also calculated the An(VI)/An(V) reduction potentials, to be discussed in the next section.

Geometric parameters for the complexes along with the corresponding population bond orders are provided in the Table 6. In general, the conformation of the neptunyl and plutonyl complexes is similar to that for uranyl–nonplanar saddle-distorted for ligand **1** and twist for ligand **2**.

Actinide–oxygen bond lengths decrease for both actinyl(V) and -(VI) with the increase of the actinide atomic number. Despite that, the corresponding bond orders slightly decrease as well, as a result of the actinide contraction. This trend is similar to what has been observed earlier for the actinyl water complexes $[\text{AnO}_2(\text{H}_2\text{O})_5]^{n+}$.^{31,70}

In general, An–N bond lengths and orders for Np and Pu follow trends described above for uranyl complexes. For the An(VI) complexes, the actinide–pyrrolic nitrogen distances decrease for both $\text{AnO}_2\mathbf{1}$ and $\text{AnO}_2\mathbf{2}$ complexes in the row $\text{U} > \text{Np} > \text{Pu}$. However, in the case of the An(V) complexes, this distance increases. Accordingly, the bond orders for An(V)–N decrease in the row $\text{U} > \text{Np} > \text{Pu}$, whereas for An(VI) they stay the same or even slightly increase.

For the alaskaphyrin complexes, metal-to-Schiff-base-nitrogen distances decrease along the actinide series (U–Np–Pu) for the actinide(VI) complexes but increase for the actinides(V). For the bi-pyren complexes, all these distances increase, but for the actinide(V) species the effect is more pronounced. The corresponding bond orders change accordingly, decreasing more strongly for the An(V) species.

TABLE 6: Selected Bond Lengths, Å, and Bond Orders for AnO₂ⁿ⁺, n = 1, 2, Complexes with Ligands 1 and 2; PBE, AE-DZP

complex	O		N1		N2		N3		N4		N5		N6	
	bond length	bond order												
U ^{VI} O ₂ 1	1.799	2.38	2.473	0.52	2.714	0.37	2.713	0.37	2.473	0.52	2.713	0.37	2.713	0.37
U ^{VO} O ₂ 1 ⁻	1.808	2.38	2.481	0.53	2.724	0.39	2.754	0.37	2.481	0.53	2.723	0.39	2.753	0.37
Np ^{VI} O ₂ 1	1.780	2.37	2.459	0.52	2.703	0.37	2.703	0.36	2.459	0.52	2.703	0.37	2.703	0.36
Np ^{VO} O ₂ 1 ⁻	1.806	2.36	2.486	0.49	2.774	0.32	2.736	0.34	2.486	0.49	2.774	0.32	2.735	0.34
Pu ^{VI} O ₂ 1	1.777	2.34	2.452	0.52	2.709	0.36	2.708	0.36	2.452	0.52	2.719	0.34	2.719	0.34
Pu ^{VO} O ₂ 1 ⁻	1.806	2.34	2.503	0.42	2.764	0.29	2.769	0.29	2.478	0.46	2.769	0.29	2.764	0.29
U ^{VI} O ₂ 2	1.801	2.38	2.484	0.53	2.687	0.39	2.688	0.4	2.484	0.53	2.688	0.4	2.688	0.4
U ^{VO} O ₂ 2 ⁻	1.830	2.37	2.508	0.51	2.710	0.4	2.701	0.4	2.514	0.5	2.701	0.4	2.710	0.4
Np ^{VI} O ₂ 2	1.782	2.37	2.470	0.53	2.689	0.39	2.689	0.39	2.470	0.53	2.689	0.39	2.689	0.39
Np ^{VO} O ₂ 2 ⁻	1.828	2.36	2.520	0.44	2.729	0.33	2.722	0.34	2.521	0.44	2.722	0.34	2.729	0.33
Pu ^{VI} O ₂ 2	1.780	2.33	2.460	0.54	2.691	0.37	2.691	0.37	2.460	0.54	2.691	0.37	2.690	0.37
Pu ^{VO} O ₂ 2 ⁻	1.821	2.34	2.522	0.4	2.735	0.29	2.736	0.29	2.522	0.4	2.736	0.29	2.736	0.29

TABLE 7: AnO₂²⁺ and Ligand Anion Formation Energies, AnO₂(V)/AnO₂(VI) Reduction Energies, Hirshfield Charges and Spin Densities on Selected Atoms, and Actinyl Stretching Vibrational Frequencies (cm⁻¹). PBE, AE-DZP

complex	<i>E</i> (1), kcal/mol	$\Delta G(\text{VI}-\text{V})$, kcal/mol	<i>q</i> (An)	<i>q</i> (O)	<i>q</i> (AnO ₂)	spin An	change in <i>q</i> (AnO ₂)(VI-V)	change in spin on An VI-V	<i>v</i> _{symm} (AnO ₂)	<i>v</i> _{asymm} (AnO ₂)
U ^{VI} O ₂ 1	-651.6		0.375	-0.282	-0.190	0.000			832	913
U ^{VO} O ₂ 1 ⁻	-345.2	-41.01	0.332	-0.309	-0.285	0.173	-0.095	0.173	788	896
Np ^{VI} O ₂ 1	-645.5		0.302	-0.257	-0.213	1.133			825	924
Np ^{VO} O ₂ 1 ⁻	-329.4	-46.79	0.203	-0.313	-0.423	1.671	-0.211	0.538	760	874
Pu ^{VI} O ₂ 1	-643.4		0.249	-0.229	-0.210	2.358			795	910
Pu ^{VO} O ₂ 1 ⁻	-323.0	-54.02	0.109	-0.312	-0.514	3.041	-0.304	0.683	742	852
U ^{VI} O ₂ 2	-693.4		0.402	-0.291	-0.181	0.000			829	908
U ^{VO} O ₂ 2 ⁻	-369.9	-25.54	0.296	-0.347	-0.397	0.476	-0.216	0.476	743	857
Np ^{VI} O ₂ 2	-686.1		0.337	-0.263	-0.188	1.102			824	915
Np ^{VO} O ₂ 2 ⁻	-358.6	-36.09	0.169	-0.352	-0.536	1.945	-0.348	0.843	724	836
Pu ^{VI} O ₂ 2	-683.8		0.287	-0.232	-0.177	2.281			800	906
Pu ^{VO} O ₂ 2 ⁻	-355.5	-46.60	0.094	-0.342	-0.591	3.213	-0.414	0.932	743	823

This picture is difficult to rationalize because many factors might have an influence on it: First, the cyclic, elliptical-shaped structure of the macrocyclic ligand, especially for the less flexible alaskaphyrin **1**, would require the An-to-Schiff-N distances to increase with the increase of the An-to-pyrrol-N distances (and vice versa). Second, the atomic radii for the metals considered decrease due to the actinide contraction. The ability of the metal orbitals, especially f-orbitals, to participate in covalent bonding would decrease as well.

The energies of reaction 1 for the actinyl complexes, provided in Table 7, show a decrease with increasing actinide atomic number for both actinyls(V) and -(VI). The same explanation as discussed above applies here as well.

It is interesting to look at charge and spin distributions as a function of the actinide atom number; the corresponding Hirshfield values are provided in Table 7. For the complexes of neptunium and plutonium, the absolute values of the charges on An and oxygen atoms decrease as compared to the uranium complexes. I.e., there is less charge separation in actinyls for the heavier metals. It can be explained by the lowering of the f-orbitals of the metal atom due to the actinide contraction, which makes them closer in the energy to the p-orbitals of the oxygens, therefore reducing charge transfer from the former to the latter.

The overall charge on the actinyl fragment (Table 7) gets substantially more negative in the series U > Np > Pu for the complexes of An(V), but not for the An(VI) complexes where differences are smaller and the charge on the Np is the most negative. The decrease of the actinide charge is a third factor, which makes the electrostatic attraction between the metal and equatorial nitrogen atoms weaker and the nitrogen–nitrogen repulsion stronger, favoring more “sparse” structures of the complex.

The extra electron added upon reduction of the An(VI) species decreases the positive charge on the actinide atom and increases the negative charge on the oxygen atoms; in the row U > Np > Pu the increase of the negative charge on the actinyl fragment gets stronger. The changes in the spin density on the actinide atom also follow this trend: Although for uranium only a fraction of the extra electron is located on the metal atom, for the plutonium complexes of **2** the extra spin density goes to the metal almost entirely. This might be evidence of decreasing f-orbital participation in the bonding and therefore greater localization of the f-electrons of actinide atoms for the higher actinides Np, Pu as compared to uranium.

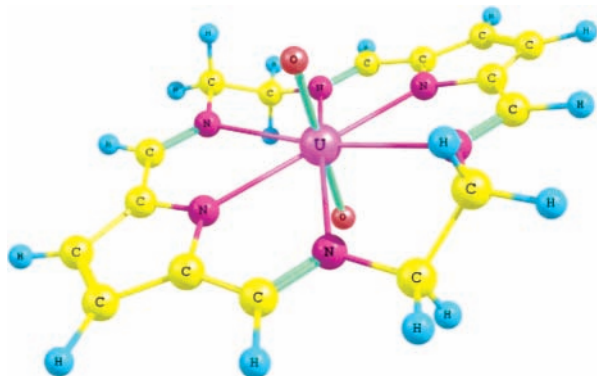
As was mentioned above for the uranium (AE-TZP) results, ligand **2** has a smaller ability of delocalizing electrons than **1**. For that reason the changes in the actinyl charge and spin density on the actinide atom during the reduction reaction eq 5 are more pronounced for the former than for the latter.

Actinyl Vibrational Frequencies. Uranyl vibrational frequencies, calculated for the alaskaphyrin dioxouranium(VI) complex by a variety of methods (Table 2) shows that all PBE calculations, AE-TZP, ADF ZORA and SC-ECP, are very close. Asymmetric uranyl(VI) stretching frequencies, available from the experiment, are reproduced better by PBE calculations than by hybrid B3LYP ones; the latter shows strong overbinding. Inclusion of the methoxy substituents lowers the uranyl frequencies and makes the agreement with experiment for PBE AE-TZP as good as within 8 cm⁻¹ difference. One can see that the AE-DZP values for uranium complexes provided in Table 7 are close to those by AE-TZP in Tables 2 and 3. A similar pattern of agreement between the experimental (IR/Raman) and theoretical (AE-DZP and AE-TZP with PBE; Gaussian03-SC-ECP with PBE or B3LYP) uranyl stretching frequencies was observed for the actinyl aquo-complexes in our previous work.³¹

TABLE 8: Reduction Potentials for the Uranyl Complexes of Alaskaphyrin 1, Bi-pyren 2 and Bi-tpmd 3

complex	$\Delta G(\text{VI}-\text{V})^a$	$\Delta\Delta G_{\text{solv}}^b$	$\Delta G(\text{VI}-\text{V})_{\text{solv}}^c$	red/ox vs FC ^c	+Hay correction ^d	experiment ^e
U ^{VI} O ₂ 1	-45.3	-41.5	-86.8	-1.20	-0.89	-0.85
U ^{VI} O ₂ 2	-31.2	-45.0	-76.2	-1.66	-1.35	-1.02
U ^{VI} O ₂ 3	-32.7	-45.9	-78.6	-1.55	-1.24	-0.96

^a AE-DZP. ^b ADF Cosmo. ^c The ferrocene (FC-Cp₂Fe⁺/Cp₂Fe) half-reaction potential is calculated to be -4.96 eV under the same conditions. ^d -0.31 eV, taken from ref 70. ^e Reference 7.

**Figure 5.** Complex UO₂2, AE-TZP geometry.

Values for complexes of different ligands, provided in Table 3, show that vibrational frequencies are slightly overestimated by the AE-TZP PBE method, but the experimental trend in the uranyl asymmetric stretch values, UO₂1 > UO₂2 = UO₂3 is reproduced correctly.

(We note that observed agreement between calculated gas-phase frequencies and experimental frequencies in real media might be in part fortuitous due to errors of the PBE method compensating matrix effects. Moreover, frequencies are calculated in the harmonic approximation, and to be completely strict in comparing with experimental frequencies, anharmonic corrections should be estimated. The anharmonic effects usually lower frequencies as compared to harmonic ones. However, it was shown⁷¹ that for bare uranyl dication stretches, the effect is rather small, about 10 cm⁻¹. So the agreement is still reasonably good.)

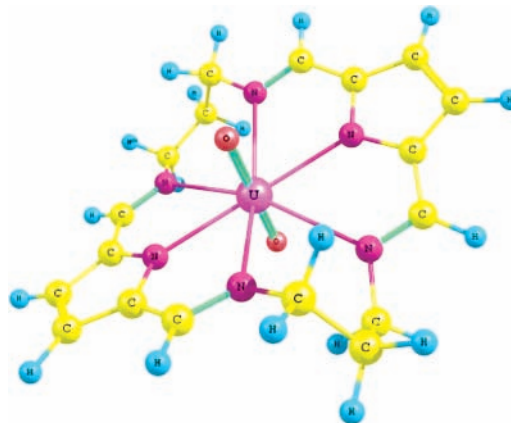
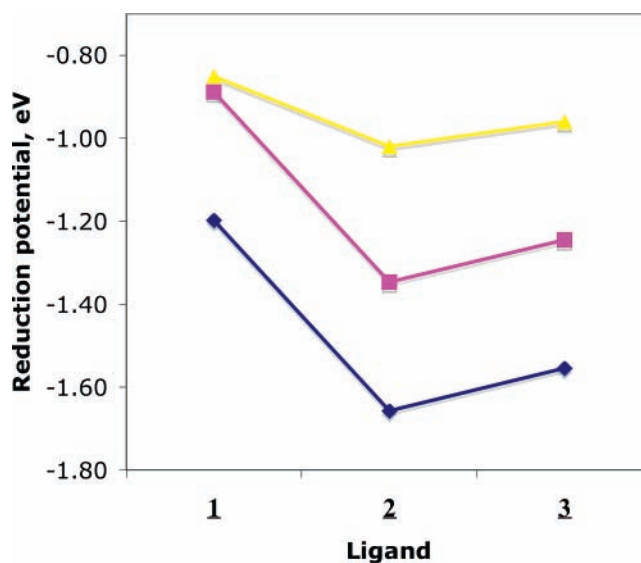
Frequencies for actinyls(V) are systematically lower than those for actinyls(VI) (Tables 3 and 7). For the actinide(V) complexes the uranyl stretching frequencies are decreasing in the row U > Np > Pu; actinide-oxygen bond lengths decrease as well, so bonds become shorter and weaker, as a result of the actinide contraction. For actinides(VI) there is not such a clear picture; wavenumbers for the uranyl stretches are slightly lower than the ones for neptunyl.

Reduction Potentials of Actinyl Complexes. Sessler et al.⁷ provide experimental electrochemical data, which gives us an opportunity to further test our methodology. Results of the calculations are provided in Table 8.

First, because we have optimized geometries for both uranyl-(V) and -(VI) complexes, we can readily calculate readily gas-phase free energies for the reduction half-reaction



Then, effects of the dichloromethane solvent on the energies were estimated using the COSMO solvation model (see the computational details section). Because reduction of neutral uranyl(VI) complexes leads to negatively charged complexes of uranyl(V), which are solvated more strongly, $\Delta\Delta G_{\text{solv}}$ are negative. One can see that both gas-phase ΔG and solvation effects are pretty much the same for complexes of 2 and 3. The alaskaphyrin ligand 1 stabilizes uranium(V) more strongly due

**Figure 6.** Complex UO₂3, AE-TZP geometry.**Figure 7.** Calculated (without (blue) and with (violet) “Hay correction”) and experimental (yellow) reduction potentials of the uranyl complexes of ligands 1–3, relative to the ferrocene couple. ADF ZORA COSMO//AE-TZP, CH₂Cl₂ solution.

to π -system delocalization of the extra electron; this also leads to a smaller solvation free energy difference. The experimental trend of 2 > 3 > 1 is adequately reproduced by the scalar relativistic calculation.

As has been shown for actinyl aquocomplexes,^{31,70} approximate single-reference DFT methods cannot describe the An(VI)/An(V) reduction potentials properly because of the importance of nondynamic correlation and spin-orbit effects. However, comparison of trends is still worthwhile because, at least for the weak ligand field case, these effects are localized in the nonbonding *f*-electron space of the metal. Moreover, they can be crudely estimated by applying a simple ad-hoc correction obtained for bare plutonyl with different numbers of *f*-electrons.⁷⁰

Inclusion of these ad-hoc corrections⁷⁰ (termed “Hay corrections” in Table 8) to account for spin-orbit and multiplet effects,

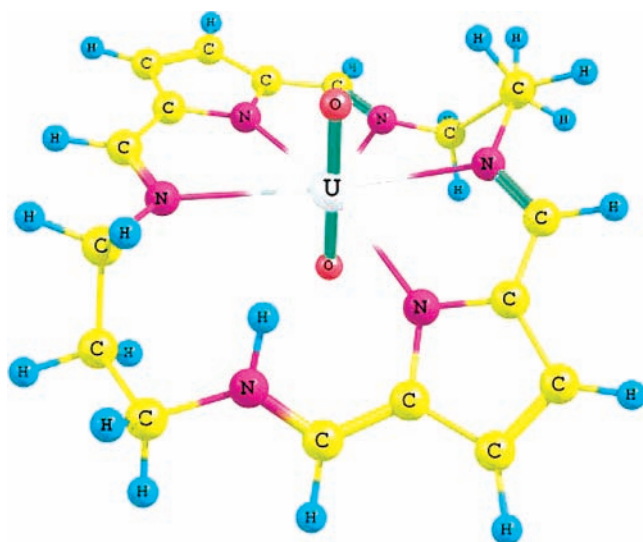


Figure 8. Complex $\text{UO}_2(3\text{H}^+)$, Schiff nitrogen protonated form, AE-TZP geometry.

which for the uranyl half reaction were estimated as -0.31 eV, shifts the results in the right direction and leads to almost quantitative agreement between theory and experiment, Table 8. The resulting reduction potentials, calculated and experimental, are provided in Figure 7. The good agreement in both trends and absolute values obtained by our procedure is encouraging. Therefore, it is worth trying to calculate reduction energies for the rest of actinyl complexes, i.e., those of neptunium and plutonium: Even if we cannot describe spin-orbit effects correctly, the procedure we use seems to be able to correctly describe the role and influence of the ligand.

It is known from the literature⁵ that, regardless of the initial state of Np and Pu, they do form complexes with alaskaphyrin (as well as other expanded porphyrin ligands) in the form of actinyl(V). In Table 7 we provide gas-phase free energies of the reduction half-reaction. One can see (Table 7) that for the gas-phase energies of the reduction, changes in the row U–Np–Pu are bigger for the bi-pyren complexes than for the alaskaphyrin one. At the same time, the values for the latter are more negative. Therefore, the choice of ligand can possibly be important in stabilizing a particular complex with a particular oxidation state, although there is no simple set of rules that would follow from our investigations.

Conclusions

In this study, we have used different modern quantum-chemical methods to study the complexes formed between actinyls AnO_2^{n+} , $n = 1$ or 2, and Schiff-base macrocyclic ligands. The agreement between the different approaches as well as comparison to the available experimental data (such as geometries, vibrational frequencies and reduction potentials) gives us strong confidence in the validity and accuracy of our methodology. We have analyzed in detail the energetics and character of bonding in the uranyl complexes of the Schiff-base macrocycles alaskaphyrin **1**, bi-pyren **2** and bi-tpmd **3**.

The uranyl complexes of alaskaphyrin **1** are predicted to be nonplanar, of C_{2v} symmetry by all our methods (PBE with scalar four-component, ZORA, small-core ECPs relativistic effects treatment, and B3LYP with SC-ECP.) This is different from the planar D_{2h} structure given by X-ray experiment. Because all the methods give a similar complex configuration, we believe that the planar structure observed in the experiment is a result of crystal packing forces. The elliptical shape of the inner cavity

of the ligand seems to be unfavorable because of too short uranium to pyrrolic nitrogens distances, and too long uranium to Schiff-base nitrogens distances. The saddle-type distortion of the ligand in the uranyl complex reflects that.

The uranyl complexes of bi-tpmd **3**, according to our scalar four-component relativistic calculations, show a five-coordination mode instead of the more symmetric six-coordinated mode given by the X-ray experiments. However, our observation allows us to explain the existing experimental data on the demetalation of uranyl complexes (namely, differences in demetalation rates between the uranyl complexes of **2** and **3**). This might be a hint that the solution geometry of $\text{UO}_2(3)$ must be closer to our gas-phase results than to that of the crystal-packed structure.

Our calculations show that among the ligands studied, the nonplanar, twist-shaped bi-pyren ligand **2** has the largest affinity to uranyl(VI) with respect to both reactions 1 and 2. The ETS energy analysis, made under the assumption of ligand and uranyl ionic fragments, explains that by the better electrostatic interaction term for **2**. The flexibility of ligands **2** and **3**, which allows for uranyl complex distortion from planarity and concomitant shortening of the metal to the Schiff-base nitrogens distances, makes the electrostatic interaction term more negative. Deviations (at least reasonably small ones) from the planar arrangement of the ligand donor atoms in the uranyl equatorial plane were found to have no substantial negative impact on the formation energy.

It shall be noted that (with the exception of the geometric parameters affected by the differences in conformation) the geometries of all the complexes, as well as their uranyl vibrational frequencies, show good agreement with the experiment. Moreover, calculated reduction potentials for the uranyl complexes of alaskaphyrin, bi-pyren and bi-tpmd correctly reproduce the experimental trends as well as the absolute values.

For the first time, we have investigated the complexes of uranyl, neptunyl and plutonyl, both (V) and (VI), with both the alaskaphyrin and bi-pyren ligands using accurate quantum-chemical methods. The affinities of these ligands to the metals is found to decrease in the row U > Np > Pu for both oxidation states of the actinyl cations. We believe that this is a direct result of the actinide contraction. The gas-phase reduction energies calculated for these complexes show that though the alaskaphyrin ligand favors the oxidation state (V) stronger than the bi-pyren ligand, the change in the reduction energy in the row U > Np > Pu is more pronounced for the latter ligand.

Acknowledgment. We are grateful to Dr. Dimitri Laikov, Moscow/Stockholm, for providing us with the Priroda code, and also for the critical reading of the manuscript. Financial support from the Natural Sciences and Engineering Research Council of Canada (NSERC) and from the University of Manitoba (start-up funds and University of Manitoba Research Grants Program) is gratefully acknowledged.

Supporting Information Available: Basis-set dependence of the formation energies from the ligand and uranyl ions, as well as uranyl(IV) and ligand radicals, is discussed in the supported information. Corresponding data are provided in Tables S1 and S2. This material is available free of charge via the Internet at <http://pubs.acs.org>.

References and Notes

- (1) Choppin, G. R. *J. Alloy. Compd.* **2002**, *344*, 55.
- (2) Ionova, G. V.; Russ, J. *Coord. Chem.* **2002**, *28*, 237.

- (3) Sessler, J. L. *Expanded, Contracted & Isomeric Porphyrins*; Pergamon Press: New York, 1997.
- (4) Sessler, J. L.; Vivian, A. E.; Seidel, D.; Burrell, A. K.; Hoehner, M.; Mody, T. D.; Gebauer, A.; Weghorn, S. J.; Lynch, V. *Coord. Chem. Rev.* **2001**, *216*, 411.
- (5) Sessler, J. L.; Gordon, A. E. V.; Seidel, D.; Hannah, S.; Lynch, V.; Gordon, P. L.; Donohoe, R. J.; Tait, C. D.; Keogh, D. W. *Inorg. Chim. Acta* **2002**, *341*, 54.
- (6) Sessler, J. L.; Mody, T. D.; Lynch, V. *Inorg. Chem.* **1992**, *31*, 529.
- (7) Sessler, J. L.; Mody, T. D.; Dulay, M. T.; Espinoza, R.; Lynch, V. *Inorg. Chim. Acta* **1996**, *246*, 23.
- (8) Katayev, E. A.; Reshetova, M. D.; Ustynyuk, Y. A. *Russ. Chem. Bull.* **2004**, *53*, 335.
- (9) Schreckenbach, G.; Hay, P. J.; Martin, R. L. *J. Comput. Chem.* **1999**, *20*, 70.
- (10) Kaltsoyannis, N. *Chem. Soc. Rev.* **2003**, *32*, 9.
- (11) Koch, W.; Holthausen, M. C. *A Chemist's Guide to Density Functional Theory*; Verlag Chemie: New York, 2000.
- (12) van Lenthe, E.; Baerends, E. J.; Snijders, J. G. *J. Chem. Phys.* **1993**, *99*, 4597.
- (13) van Lenthe, E.; Baerends, E. J.; Snijders, J. G. *J. Chem. Phys.* **1994**, *101*, 9783.
- (14) van Lenthe, E.; Ehlers, A.; Baerends, E. J. *J. Chem. Phys.* **1999**, *110*, 8943.
- (15) Küchle, W.; Dolg, M.; Stoll, H.; Preuss, H. *J. Chem. Phys.* **1994**, *100*, 7535.
- (16) Laikov, D. N. An implementation of the scalar relativistic density functional theory for molecular calculations with Gaussian basis sets. DFT2000 Conference, Menton, France, 2000.
- (17) Clavaguera-Sarrio, C.; Hoyau, S.; Ismail, N.; Marsden, C. J. *J. Phys. Chem. A* **2003**, *107*, 4515.
- (18) Cao, X. Y.; Dolg, M. *Mol. Phys.* **2003**, *101*, 2427.
- (19) Brynda, M.; Wesolowski, T. A.; Wojciechowski, K. *J. Phys. Chem. A* **2004**, *108*, 5091.
- (20) Chernyadyev, A. Y.; et al. *Russ. Chem. Bull.* **2001**, *50*, 2445.
- (21) Liao, M. S.; Kar, T.; Scheiner, S. *J. Phys. Chem. A* **2004**, *108*, 3056.
- (22) Snijders, J. G.; Baerends, E. J.; Ros, P. *Mol. Phys.* **1979**, *38*, 1909.
- (23) Boerrigter, P. M.; Baerends, E. J.; Snijders, J. G. *Chem. Phys.* **1988**, *122*, 357.
- (24) Ziegler, T.; Tschinke, V.; Baerends, E. J.; Snijders, J. G.; Ravenek, W. *J. Phys. Chem.* **1989**, *93*, 3050.
- (25) Laikov, D. N. *Chem. Phys. Lett.* **1997**, *281*, 151.
- (26) Laikov, D. N. Priroda code.
- (27) Dyall, K. G. *J. Chem. Phys.* **1994**, *100*, 2118.
- (28) Perdew, J. P.; Burke, K.; Ernzerhof, M. *Phys. Rev. Lett.* **1996**, *77*, 3865.
- (29) Laikov, D. N. *Chem. Phys. Lett.* **2005**, *416*, 116.
- (30) Shamov, G. A.; Laikov, D. N.; Schreckenbach, G.; Vo, T. To be published.
- (31) Shamov, G. A.; Schreckenbach, G. *J. Phys. Chem. A* **2005**, *109*, 10961.
- (32) Frisch, M. J.; Trucks, G. W.; Schlegel, H. B.; Scuseria, G. E.; Robb, M. A.; Cheeseman, J. R.; Montgomery, J. A., Jr.; Vreven, T.; Kudin, K. N.; Burant, J. C.; Millam, J. M.; Iyengar, S. S.; Tomasi, J.; Barone, V.; Mennucci, B.; Cossi, M.; Scalmani, G.; Rega, N.; Petersson, G. A.; Nakatsuji, H.; Hada, M.; Ehara, M.; Toyota, K.; Fukuda, R.; Hasegawa, J.; Ishida, M.; Nakajima, T.; Honda, Y.; Kitao, O.; Nakai, H.; Klene, M.; Li, X.; Knox, J. E.; Hratchian, H. P.; Cross, J. B.; Bakken, V.; Adamo, C.; Jaramillo, J.; Gomperts, R.; Stratmann, R. E.; Yazyev, O.; Austin, A. J.; Cammi, R.; Pomelli, C.; Ochterski, J. W.; Ayala, P. Y.; Morokuma, K.; Voth, G. A.; Salvador, P.; Dannenberg, J. J.; Zakrzewski, V. G.; Dapprich, S.; Daniels, A. D.; Strain, M. C.; Farkas, O.; Malick, D. K.; Rabuck, A. D.; Raghavachari, K.; Foresman, J. B.; Ortiz, J. V.; Cui, Q.; Baboul, A. G.; Clifford, S.; Cioslowski, J.; Stefanov, B. B.; Liu, G.; Liashenko, A.; Piskorz, P.; Komaromi, I.; Martin, R. L.; Fox, D. J.; Keith, T.; Al-Laham, M. A.; Peng, C. Y.; Nanayakkara, A.; Challacombe, M.; Gill, P. M. W.; Johnson, B.; Chen, W.; Wong, M. W.; Gonzalez, C.; Pople, J. A. *Gaussian 03*; Gaussian, Inc.: Wallingford, CT, 2004.
- (33) Batista, E. R.; Martin, R. L.; Hay, P. J.; Peralta, J. E.; Scuseria, G. E. *J. Chem. Phys.* **2004**, *121*, 2144.
- (34) Becke, A. D. *J. Chem. Phys.* **1993**, *98*, 5648.
- (35) Lee, C.; Yang, W.; Parr, R. G. *Phys. Rev. B: Condens. Matter* **1988**, *37*, 785.
- (36) Stephens, P. J.; Devlin, F. J.; Chabalowski, C. F.; Frisch, M. J. *J. Phys. Chem.* **1994**, *98*, 11623.
- (37) Fonseca Guerra, C.; Visser, O.; Snijders, J. G.; te Velde, G.; Baerends, E. J. Parallelisation of the Amsterdam Density Functional Program. In *Methods and Techniques in Computational Chemistry ME-TECC-95*; Clementi, E., Corongiu, C., Eds.; STEF: Cagliari, Italy, 1995; p 305.
- (38) te Velde, G.; Bickelhaupt, F. M.; Baerends, E. J.; Fonseca Guerra, C.; van Gisbergen, S. J. A.; Snijders, J. G.; Ziegler, T. *J. Comput. Chem.* **2001**, *22*, 931.
- (39) Baerends, E. J.; et al. *ADF 2004.01: Scientific Computing and Modelling, Theoretical Chemistry*; Vrije Universiteit: Amsterdam, The Netherlands, 2004.
- (40) Morokuma, K.; Kitaura, K. Energy decomposition analysis of molecular interactions. In *Chemical applications of atomic and molecular electrostatic potentials*; Politzer, P., Truhlar, D. G., Eds.; Plenum: New York, 1981; p 215.
- (41) Ziegler, T.; Rauk, A. *Theor. Chim. Acta* **1977**, *46*, 1.
- (42) Ziegler, T.; Rauk, A. *Inorg. Chem.* **1979**, *18*, 1558.
- (43) Bickelhaupt, F. M.; Baerends, E. J. In *Reviews in Computational Chemistry*; Wiley: New York, 2000; Vol. 15; p 1.
- (44) Klamt, A.; Schüürmann, G. *J. Chem. Soc., Perkin Trans.* **1993**, *2*, 799.
- (45) Pye, C. C.; Ziegler, T. *Theor. Chem. Acc.* **1999**, *101*, 396.
- (46) Klamt, A.; Jonas, V.; Bürger, T.; Lohrenz, J. C. W. *J. Phys. Chem. A* **1998**, *102*, 5074.
- (47) Denning, R. G. *Struct. Bonding (Berlin)* **1992**, *79*, 215.
- (48) Ionova, G. V.; Pershina, V. G.; Suraeva, N. I. *Russ. J. Inorg. Chem.* **1991**, *36*, 175.
- (49) Maron, L.; Leininger, T.; Schimmelpfennig, B.; Vallet, V.; Heully, J. L.; Teichteil, C.; Groen, O.; Wahlgren, U. *Chem. Phys.* **1999**, *244*, 195.
- (50) Clavaguera-Sarrio, C.; Vallet, V.; Maynau, D.; Marsden, C. J. *J. Chem. Phys.* **2004**, *121*, 5312.
- (51) Gagliardi, L. A.; Roos, B. O. *Chem. Phys. Lett.* **2000**, *331*, 229.
- (52) Zhou, M. F.; Andrews, L.; Ismail, N.; Marsden, C. J. *J. Phys. Chem. A* **2000**, *104*, 5495.
- (53) Han, Y.-K.; Hirao, K. *J. Chem. Phys.* **2000**, *113*, 7345.
- (54) Dyall, K. G. *Mol. Phys.* **1999**, *96*, 511.
- (55) Schreckenbach, G.; Hay, P. J.; Martin, R. L. *Inorg. Chem.* **1998**, *37*, 4442.
- (56) Denning, R. G. *J. Chem. Phys.* **2002**, *117*, 8008.
- (57) Kovacs, A.; Konings, R. J. M. *J. Mol. Struct. (THEOCHEM)* **2004**, *684*, 35.
- (58) Hirshfeld, F. L. *Theor. Chim. Acta* **1977**, *44*, 129.
- (59) Wiberg, K. B.; Rablen, P. R. *J. Comput. Chem.* **1993**, *14*, 1504.
- (60) Mayer, I. *Simple theorems, proofs, and derivations in quantum chemistry*; Kluwer Academic/Plenum Publishers: New York, 2003.
- (61) Atanasov, M.; Daul, C. A.; Fowe, E. P. *Monatsh. Chem.* **2005**, *136*, 925.
- (62) Bridgeman, A. J.; Cavigliasso, G.; Ireland, L. R.; Rothery, J. J. *Chem. Soc., Dalton Trans.* **2001**, 2095.
- (63) Clark, A. E.; Sonnenberg, J. L.; Hay, P. J.; Martin, R. L. *J. Chem. Phys.* **2004**, *121*, 2563.
- (64) Bridgeman, A. J.; Cavigliasso, G. *Faraday Discuss.* **2003**, *124*, 239.
- (65) Ernzerhof, M.; Scuseria, G. E. *J. Chem. Phys.* **1999**, *110*, 5029.
- (66) Bersuker, I. B. *Electronic Structure and Properties of Transition Metal Compounds: Introduction to the Theory*; Wiley: New York, 1996.
- (67) Shamov, G. A.; Schreckenbach, G. Unpublished results.
- (68) Frenking, G.; Wichmann, K.; Frohlich, N.; Loschen, C.; Lein, M.; Frunzke, J.; Rayon, V. M. *Coord. Chem. Rev.* **2003**, *238*, 55.
- (69) Hambright, P. Dynamic coordination chemistry of metalloporphyrins. In *Porphyrins and metalloporphyrins*; Smith, K. M., Ed.; Elsevier: New York, 1975; p 234.
- (70) Hay, P. J.; Martin, R. L.; Schreckenbach, G. *J. Phys. Chem. A* **2000**, *104*, 6259.
- (71) Clavaguera-Sarrio, C.; Ismail, N.; Marsden, C. J.; Begue, D.; Pouchan, C. *Chem. Phys.* **2004**, *302*, 1.